# POTENTIAL OF A TRANSCRITICAL REGENERATIVE SERIES TWO STAGE ORGANIC RANKINE CYCLE FOR DUAL SOURCE WASTE HEAT RECOVERY

Anandu Surendran[1]*, Satyanarayanan Seshadri[2]

[1]Department of Applied Mechanics, Indian Institute of Technology Madras
Chennai, Tamil Nadu, India
anandusurendran@smail.iitm.ac.in

[2]Department of Applied Mechanics, Indian Institute of Technology Madras
Chennai, Tamil Nadu, India
satya@iitm.ac.in

## ABSTRACT

A Transcritical Regenerative Series Two stage Organic Rankine cycle (TR-STORC) that improves on the existing Series Two stage ORC (STORC) architecture by combining supercritical heating in the high pressure (HP) stage and partial evaporation and regeneration in the low pressure (LP) stage is proposed. Exhaust gas and jacket water from a stationary IC engine is used as the primary and secondary heat source for the cycle respectively. Using cyclopentane as working fluid, the influence of cycle parameters is analysed and optimized performances for a range of operating conditions are evaluated. At lower HP evaporator pressures, lower values of vapour outlet temperatures lead to maximum power output. The optimum vapour fraction in the LP evaporator outlet decreases with the increase in vapour outlet temperature in the HP stage. Utilization rate of secondary heat source decreases linearly with LP evaporation temperature. An intermediate LP evaporation temperature exists that maximises the net power output. A constrained optimization using Genetic Algorithm is carried out for various operating conditions. At the engine design point, TR-STORC delivers 16% and 23% higher power output than STORC and pre-heated ORC respectively. For a wide range of heat source temperatures and heat ratios, TR-STORC presents excellent exergetic performance over STORC and pre-heated ORC.

## 1. INTRODUCTION

Heat recovery using Organic Rankine Cycle (ORC) is commonly employed across many applications such as IC engines, geothermal heat sources, solar thermal power systems etc...Many application of heat recovery typically involve two or more heat sources present concurrently. A common case is IC engine waste heat recovery, with dual heat sources present at different temperatures and heat contents.

In IC engines, single pressure pre-heated ORC and dual loop ORC are commonly employed (Shi *et al.*, 2018 [1]) where pre-heated ORCs report very poor utilization of the low temperature heat source (Vaja and Gambarotta,2009). Studies on dual loop ORCs by Shu *et al.* (2014) report higher exergy efficiency and heat source utilization rates, however they require separate expanders, higher heat exchanger area requirements increasing the complexity of implementation. Recent studies on dual pressure (two stage) ORC architectures shows two stage ORCs to have improved exergetic efficiency compared to single pressure ORCs (Manente *et al.*, 2017)(Li *et al.*, 2019). So far, only a few studies have focused on the use of two stage evaporation architectures for dual source heat recovery applications where maximum heat source utilization is desired. In a linked two level heat source system like the IC engine, Rech *et al.* (2017) analyzed the design and off design performance of subcritical and supercritical parallel two stage ORC (PTORC) layouts over single stage ORCs. The supercritical PTORC layout reached the best performance, achieving a thermal efficiency of 12.6%. Chen *et al.* (2017) proposed a confluent cascade expansion ORC (CCE-RC - same as PTORC) system which produced 8% more net power with 18% lower heat exchanger volume as compared to dual loop ORC. Li *et al.* (2015) compared two dual pressure architectures namely the Series two stage ORC (STORC) and PTORC. STORC presented higher exergetic performance over PTORC. Li *et al.*( 2019) proposed an improved STORC that coupled supercritical and subcritical heat absorption processes.

For heat source temperature above 135°C, the modified cycle was able to generate 20.4% increased power output than STORC. Recently, studies on partial evaporation in ORCs for low temperature single heat source applications have reported higher heat extraction and power output than fully evaporated ORCs. The improvement in cycle performance due to partial evaporation is higher for lower heat source temperatures. (Lecompte *et al.*,2015)

In this study, a new two stage ORC namely Transcritical Regenerative STORC (TR-STORC) is proposed, which is an improvement on the existing STORC architecture focusing on dual source heat recovery. TR-STORC adopts a supercritical evaporation process in the HP stage. In the LP stage, working fluid is only partially evaporated. Full evaporation of LP stage fluid is achieved by utilizing the high superheat of vapor exiting from the HP turbine. This combination of supercritical heating in the HP stage and partial evaporation and regeneration in the LP stage can improve the thermal match and can also achieve increased heat source utilization. Exhaust gas and jacket water from a 2.97 MW natural gas IC engine are the heat sources. Influence of cycle parameters are analysed and optimized performances for a range of operating conditions are evaluated. Finally, a constrained optimization using Genetic Algorithm is carried out for various operating conditions and the cycle performance is compared with STORC and the basic pre-heated ORC architecture.

## 2. SYSTEM DESCRIPTION

### 2.1 Waste heat sources

The heat source in this study is a 20 cylinder 4 stroke turbocharged natural gas fired engine used in stationary applications and operated mostly at its design point. High temperature exhaust gases (432 °C, 4.591 kg/s) from the engine is the primary heat source and the hot jacket water (90°C, 14 kg/s) is the secondary heat source. The composition of primary heat source used for determining its properties is $O_2$ 17.3%, $N_2$ 59.3%, $CO_2$ 12.9% and $H_2O$ 10.5 % by mass.

### 2.2 Cycle architecture and working principle

Figure 1 shows the layout and T-s diagram of TR-STORC. The system consists of a high pressure (HP) evaporator, a low pressure (LP) evaporator, a regenerator, a high pressure pump, a low pressure pump, a two stage induction turbine and a condenser. The high pressure and low pressure evaporators recover heat from the primary and secondary heat sources respectively. The saturated working fluid from the condenser is pressurised to an intermediate pressure by the LP pump (9-1). A part of the working fluid is pressurised to a higher pressure by the HP pump (2-4). In the LP evaporator, the working fluid absorbs heat from the secondary heat source and is partially evaporated (1-2-3). In the HP evaporator, the working fluid absorbs heat from the primary heat source and generates high pressure supercritical vapour (4-5). The high pressure vapour is expanded in the HP stage of the induction turbine (5-6).The entire vapour exiting the HP stage then mixes with working fluid from the LP evaporator and fully evaporates it in the mixer to produce low pressure saturated vapour (at 3-3” and 6-3”). This vapour is then expanded to the condenser pressure via the LP turbine (3”-7). The mechanical work from the turbine is converted to electrical power by the generator. The superheated vapour exiting the turbine is then de-superheated (7-8) and condensed to saturated liquid in the condenser (8-9). This completes one cycle.

Cyclopentane is selected as the working fluid for this study. The main properties of cyclopentane are listed in Table 1.

**Table 1:** Thermodynamic properties of cyclopentane

| Working fluid | Molecular mass (g/mol) | Normal boiling point(K) | Critical temperature $T_c$ (K) | Critical pressure $P_c$ (MPa) | GWP | ODP |
|---|---|---|---|---|---|---|
| Cyclopentane | 70.133 | 322.40 | 511.69 | 4.515 | 11 | 0 |

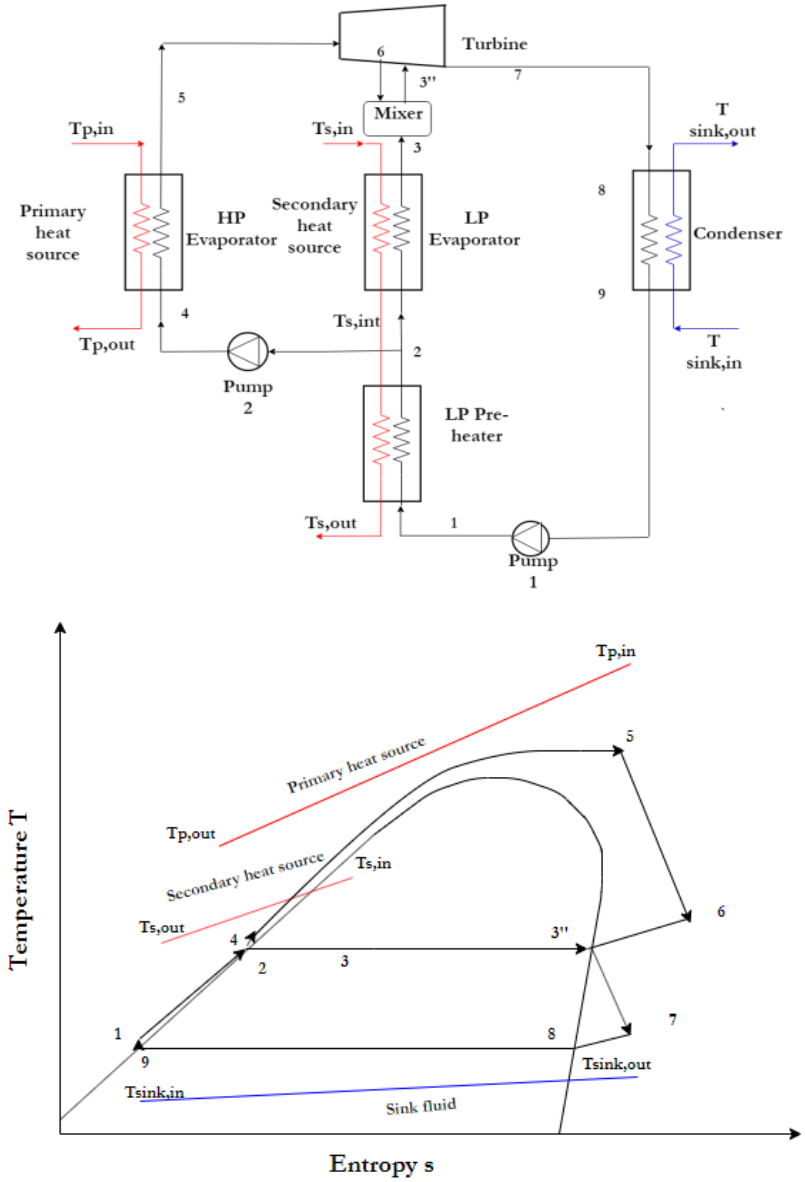


**Figure 1:** (a) TR-STORC layout (b) T-s diagram of TR-STORC

## 3. MODELLING METHODOLOGY

The ORC system is evaluated based on the following assumptions

- All processes are at steady state
- Pressure drop and heat transfer from the pipelines is neglected
- Changes in kinetic and potential energy of the working fluid is negligible
- Ambient temperature ($T_0$) and pressure ($P_0$) are assumed to be 298K and 0.1 MPa respectively
- All heat exchangers are counter flow type
- Both LP and HP turbine stages have same isentropic efficiency

The cycle parameters used in the present study are shown in Table 2. The main thermodynamic model equations are shown in Table 3.

**Table 2:** Cycle parameters

| Parameter | | Value |
|---|---|---|
| ΔT pinch HP evaporator | $\Delta T_{evap,HP}$ (K) | 20 |
| ΔT pinch LP evaporator | $\Delta T_{evap,LP}$ (K) | 10 |

| | | |
|---|---|---|
| ΔT pinch condenser | $\Delta T_{cond}$ (K) | 10 |
| Isentropic expander efficiency | $\eta_e$ (%) | 70 |
| Isentropic pump efficiency | $\eta_p$ (%) | 80 |
| Primary heat carrier pressure | $P_P$ (kPa) | 101.325 |
| Primary heat source cooling limit | $T_{P,\,outmin}$ (K) | 373 |
| Inlet temperature cooling water | $T_{sink,\,in}$ (K) | 298 |
| Outlet temperature cooling water | $T_{sink,\,out}$ (K) | 303 |

**Table 3**: Modelling equations

| Parameter | Equations |
|---|---|
| Net power output (kW) | $W_{net} = (W_{exp,HP} + W_{exp,LP}) - W_{pump,HP} - W_{pump,LP}$ |
| Thermal efficiency (%) | $\eta_I = W_{net}/Q_{total}$ |
| Total primary heat (kW) | $Q_{P,total}=C_{pP}.\, m_P.(T_{P,in}-T_0)$ |
| Total secondary heat (kW) | $Q_{S,total}=C_{pS}.\, m_S.(T_{s,in}-T_0)$ |
| Utilization rate of primary source (%) | $U_p= Q_{HP\ evap}\ /Q_{P,all}$ |
| Utilization rate of secondary source (%) | $U_S= (Q_{LP\ evap} + Q_{LP\ pre\text{-}heater})/Q_{S,all}$ |
| Exergy rate of primary heat source (kW) | $Ex_P = m_P e_P = m_P.(h_P - h_0 - T_0(s_P - s_0))$ |
| Exergy rate of secondary heat source (kW) | $Ex_S = m_S e_S = m_S.(h_S - h_0 - T_0(s_S - s_0))$ |
| Second law efficiency $\eta_{ex}$(exergetic efficiency) (%) | $\eta_{ex} = {W_{net}}/{(Ex_P+Ex_S)}$ |

The modelling of the heat exchangers is based on a discretized approach by Larsen *et al.* (2013). The primary heat source cooling limit and the pinch point temperature difference in the evaporator sets the constraint for iteratively calculating the mass flow rate $m_{wf1}$in the HP loop. The vapour fraction of the working fluid at the outlet of LP evaporator and the pinch point temperature difference determines the mass flow rate $m_{wf2}$. For dry fluids, such as cyclopentane superheating isn't necessary at the turbine inlet. The mass flow rate $m_{wf2}$ and vapour fraction is then iterated so as to achieve a saturated vapour condition at the outlet of the mixer, thereby ensuring full evaporation of working fluid from the LP loop. Based on the above assumptions and equations, a model is developed in MATLAB using thermodynamic properties of fluids from REFPROP® 9.1 software. Energy balance and mass balance is then applied across each components (as a control volume) to determine the system characteristics.

## 4. RESULTS

### 4.1 Influence of HP evaporation pressure and vapor outlet temperature

Figure 2 presents the effect of HP evaporation pressure and HP vapour outlet temperature on net power output, LP vapour fraction (at state point 3), thermal efficiency and heat source utilization rates. At lower evaporator pressures, lower values of vapour outlet temperatures lead to maximum work output. This is due to the increased first stage turbine work owing to lower superheated temperatures at the outlet of HP turbine as well as higher mass flow rates in the HP loop. As the HP stage pressure increase, the net power output also increase for a given LP stage evaporating temperature (pressure). This is due to the increase in pressure ratio across the HP turbine. The optimum vapour fraction in the LP evaporator outlet decreases with the increase in vapour outlet temperature in the HP stage. This can be attributed to the increased degree of superheat available at the exit of the HP turbine at higher vapour outlet temperatures. Also, for higher HP stage pressures the optimum vapour fraction is higher for a given vapour outlet temperature due to the decrease in available superheat at exit of HP expander.

The primary heat source utilization remains almost constant with vapour outlet temperature. The peaks in secondary heat source utilization correspond to maximum mass flow rates in the pre-heater section of LP evaporator. The variation in thermal efficiency is a direct result of the variation in net power output and heat source utilization rates for various vapour outlet temperatures and pressures

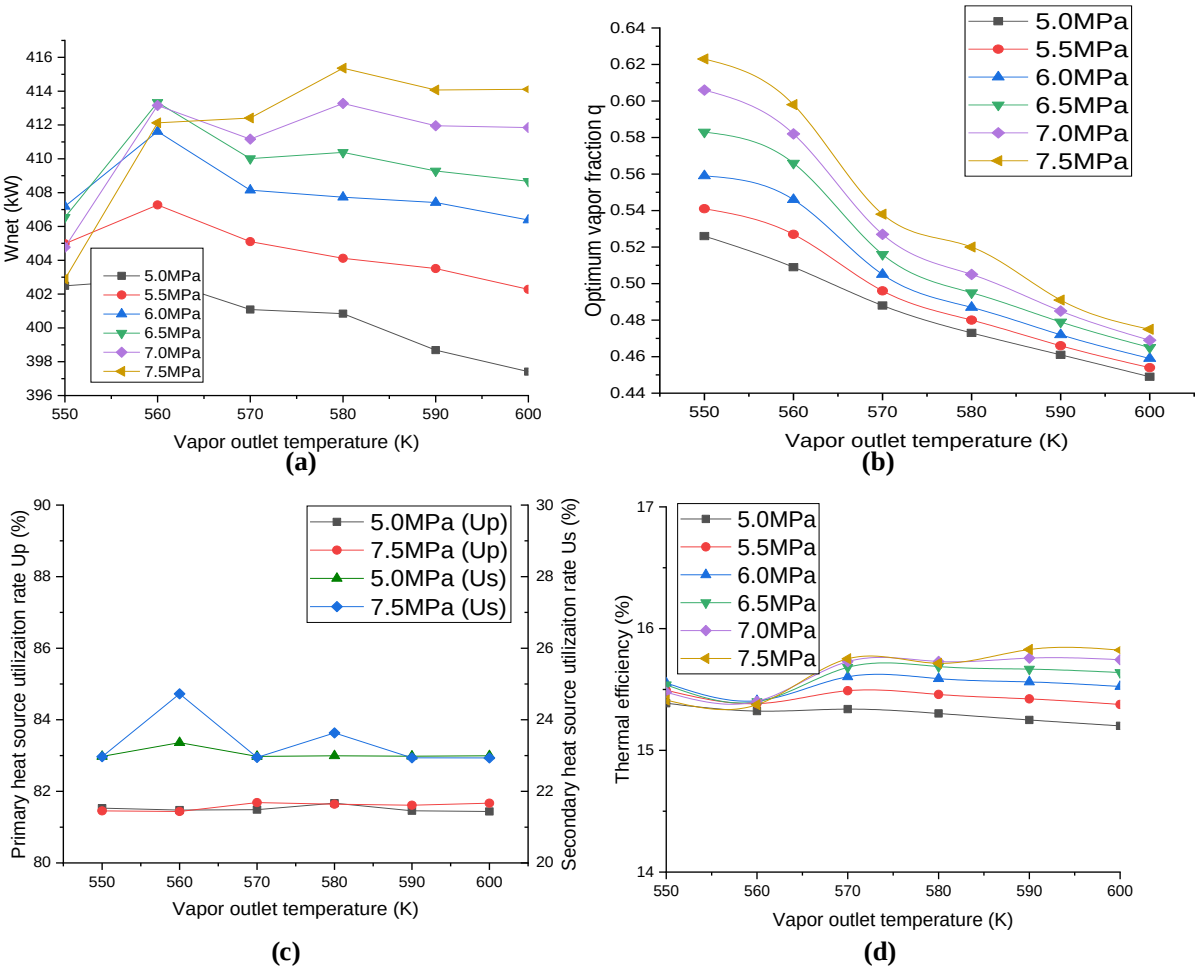


**Figure 2:** Effect of HP stage pressure and vapour outlet temperature on (a) Net power output (b) Optimum vapour fraction in the LP evaporator (c) Utilization rates of heat sources (d) Thermal efficiency. LP evaporation temperature is set to 343K.

### 4.2 Influence of LP evaporation temperature

Figure 3 presents the effect of LP evaporation temperature ($T_3$) on net power output, thermal efficiency and secondary heat source utilization rate. At lower values of $T_3$, very high utilization of secondary heat source is achieved due to the increased mass flow rate of working fluid in the LP loop. However, the irreversibility associated with mixing of superheated vapour and partially evaporated working fluid from the LP evaporator increases with decrease in LP evaporation temperature. Also, at lower values of $T_3$ the thermal efficiency of the LP stage decreases resulting in lower power outputs. Thus, for a given HP stage pressure and vapour outlet temperature, there exists an intermediate value of $T_3$ that maximizes the net power output of the TR-STORC.

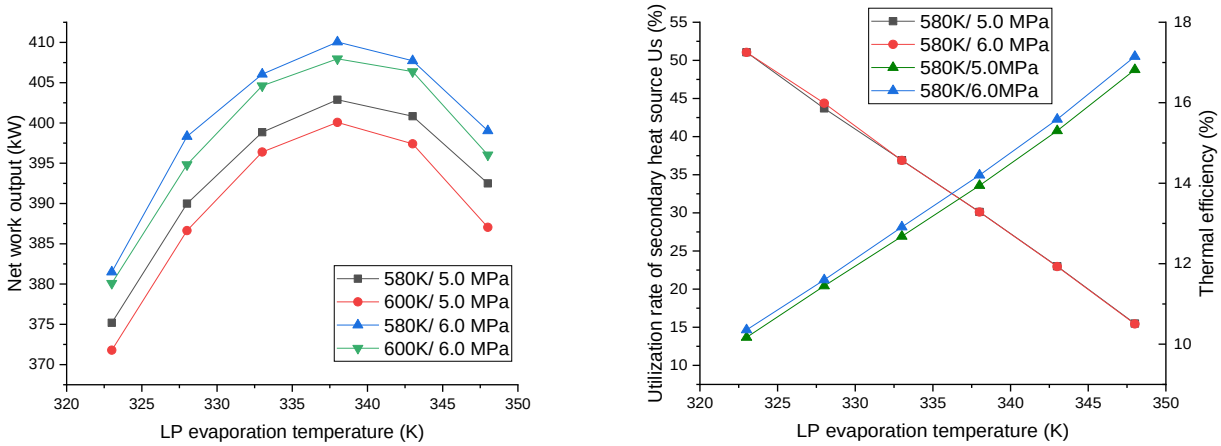

**(a)** **(b)**

**Figure 3:** Effect of LP stage evaporation temperature on (a) Net power output (b) Utilization rates of secondary heat source

### 4.3 Optimization and comparison

For the TR-STORC the optimization parameters are the HP stage pressure, the vapor outlet temperature $T_6$, the LP evaporation temperature $T_3$ and the condensation temperature. The range of optimizing parameters along with the cycle design constraints are shown in Table 4. The maximum operating temperature of the working fluid is set as the upper limit on the vapor outlet temperature. Condenser pressure is kept above atmospheric pressure to prevent air leakage into the system. Volumetric flow ratios (VFR) of both HP and LP turbines are constrained within 50 so that single stage turbines with can be used (Invernizzi *et al.*, 2007). The cooling limit on the primary heat source is set to 373K to prevent acid droplet formation. The cycle parameters are optimized using Genetic Algorithm (GA) with net power output as the objective function. The optimized cycle performance is then compared with an optimized STORC and pre-heated ORC for various cases.

**Table 4**: Optimizing parameters and constraints

| **Parameter** | **Value** |
|---|---|
| $T_6$ | 560-600K |
| $T_3$ | 323K –($T_{s,in}$ -$\Delta T_{evap,LP}$)K |
| $P_{HP\ evap}$ | 1.1 $P_c$- 8MPa |
| $T_{cond}$ | 313K-333K |
| **Constraints** | |
| $P_{cond}$ | 1.20 bar |
| VFR HP turbine | <= 50 |
| VFR LP turbine | <= 50 |
| Degree of sub cooling | 5K |
| $T_{p,out\ min}$ | 373K |
| **GA parameters** | |
| Population size | 20 |
| Maximum generations | 15 |
| Function tolerance | 0.01kW |

4.3.1 Performance at engine design point

The optimized performance of TR-STORC, STORC and pre-heated ORC at engine design point is shown in Table 5. TR-STORC delivers the highest power output which is 16% higher than STORC and 23% higher than pre-heated ORC. Among the three cycle architectures, TR-STORC also has the highest thermal efficiency. The utilization of primary heat source is almost the same for all the three architectures. STORC utilizes the secondary heat source to the highest. However, TR-STORC's improved thermal matching due to supercritical heating in HP evaporator and partial evaporation in the LP evaporator of leads to higher heat exchanger UA requirements over STORC and pre-heated ORC.

**Table 5**: Optimum cycle performances at design point

| **Parameters** | **Pre-heated ORC** | **STORC** | **TR-STORC** |
|---|---|---|---|
| $W_{net}$ (kW) | 280 | 297 | 344 |
| $\eta_I$ (%) | 14.4 | 12.2 | 15.3 |
| $\eta_{ex}$(%) | 14.2 | 15.0 | 17.4 |
| $U_p$ (%) | 81.5 | 81.6 | 81.6 |
| $U_s$ (%) | 5.20 | 18.4 | 13.3 |
| $m_{wf}$(kg/s) | 3.50 | 4.85 | 4.84 |
| $T_{evap,LP}$ (K) | - | 344 | 347 |
| $T_{evap,HP}$ (K) | 460 | 460 | 582 |

| | | | |
|---|---|---|---|
| $P_{evap,HP}$ (MPa) | 2.18 | 2.18 | 6.83 |
| $VFR_{LP}$ | - | 1.6 | 1.7 |
| $VFR_{HP}$ | 21.6 | 13.5 | 45.2 |
| UA (kW/K) | 117 | 147 | 149 |
| W/UA | 2.46 | 2.02 | 2.31 |

4.3.2 Variation with heat source temperatures

In this section, the primary and secondary heat source temperatures are varied. A parameter φ is introduced, which is the relative increase in net power output over pre-heated ORC. For the temperature ranges investigated, TR-STORC shows superior performance over pre-heated ORC and STORC. TR-STORC delivers approximately 14%-20% more power output than STORC. As the secondary heat source temperature increases, the relative increase in power output of TR-STORC and STORC exceeds that of pre-heated ORC due to the improved thermal efficiency and temperature matching in the LP stage.

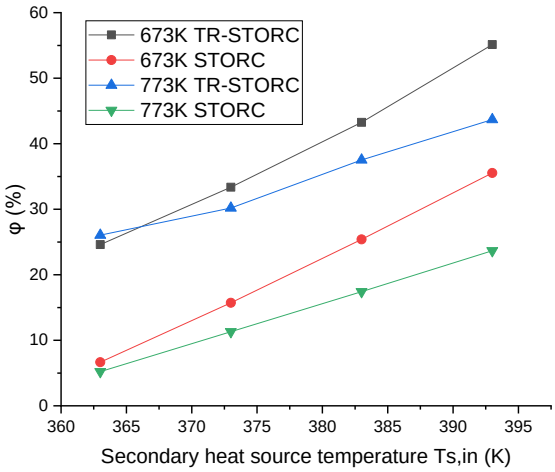


**Figure 4:** Relative increase in power output over pre-heated ORC for various heat source temperatures.

4.3.3 Variation with heat ratio

The fraction of heat available from the primary and secondary heat source is varied in this study. Typically, in dual source applications, one of the heat sources would have heat content higher than the other. Heat ratio which is the ratio of heat available from the primary heat source to the secondary heat source can be defined as:

$$Q_r = \frac{Q_P}{Q_S} = \frac{m_P \times Cp_P \times (T_{P,in} - T_{P,out\,min})}{m_S \times Cp_S \times (T_{S,in} - T_{S,out\,min})}$$

Figure5 shows the relative increase in power output over pre-heated ORC with $Q_{ratio}$ for TR-STORC and STORC.. At lower heat ratios ($Q_{ratio}$<1), there is significant heat available from the secondary heat source, which the two stage architectures are able to utilize significantly At $Q_{ratio}$<1, this improved secondary heat source utilization of two stage layout is the primary reason for the increased work output of STORC and TR-STORC over pre-heated ORC. For all heat ratios, TR-STORC outperforms STORC and the effect is seen to increase at higher heat ratios. This is due to the improved thermal match with the primary heat source in TR-STORC owing to supercritical evaporation in the HP evaporator. For the heat ratios investigated, TR-STORC delivers 4.8-5.5% increased power output than STORC.

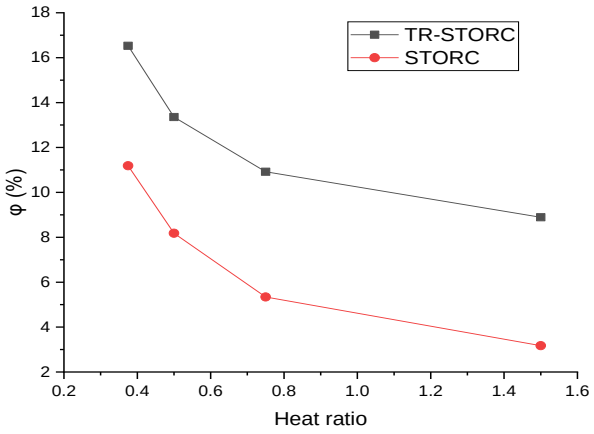


**Figure 5:** Relative increase in power output over pre-heated ORC for TR-STORC and STORC with heat ratio $Q_r$. Primary and secondary heat sources temperatures are fixed at 673K and 363K respectively.

## 5. CONCLUSION

A two stage cycle architecture that improves on the existing STORC architecture by combining supercritical heating in the HP stage and partial evaporation and regeneration in the LP stage is proposed. Exhaust gas and jacket water from an IC engine is used as the primary and secondary heat source for the cycle. Influence of cycle parameters is analysed and optimized performances for a range of operating conditions are evaluated using cyclopentane as working fluid. The main conclusions are:

1. At lower evaporator pressures, lower values of vapour outlet temperatures lead to maximum work output. The vapour fraction in the LP evaporator outlet decreases with the increase in vapour outlet temperature in the HP stage.
2. Utilization rate of secondary heat source decreases linearly with LP evaporation temperature. An intermediate LP evaporation temperature exists that maximises the net power output.
3. At the engine design point, TR-STORC delivers 16% and 23% higher power output than STORC and pre-heated ORC respectively.
4. Upon varying the heat source temperatures and heat ratios, TR-STORC presents excellent exergetic performance for dual source heat recovery over STORC and pre-heated ORC.

## NOMENCLATURE

| | | |
|---|---|---|
| $C_p$ | specific heat at constant pressure | (kJ/kg K) |
| e | specific exergy | (kJ/kg) |
| Ex | exergy | (kJ) |
| h | specific enthalpy | (kJ/kg) |
| m | mass flow rate | (kg/s) |
| P | pressure | (MPa) |
| Q | heat transfer rate | (kW) |
| s | specific entropy | (kJ/kg K) |
| T | temperature | (K) |
| U | utilization rate of heat source | (%) |
| UA | thermal conductance | (kW/K) |
| W | power | (kW) |

**Subscript**

| | |
|---|---|
| cond | condenser |
| evap | evaporator |
| exp | expander |
| HP | high pressure |
| in | inlet |
| LP | low pressure |
| max | maximum |
| min | minimum |
| out | outlet |
| P | primary |
| r | ratio |
| S | secondary |
| wf | working fluid |

## REFERENCES

L. Shi, G. Shu, H. Tian, and S. Deng, "A review of modified Organic Rankine cycles (ORCs) for internal combustion engine waste heat recovery (ICE-WHR)," *Renew. Sustain. Energy Rev.*, vol. 92, pp. 95–110, Sep. 2018.

I. Vaja and A. Gambarotta, "Internal Combustion Engine ( ICE ) bottoming with Organic Rankine Cycles ( ORCs )," *Energy*, vol. 35, no. 2, pp. 1084–1093, 2010.

G. Shu, L. Liu, H. Tian, H. Wei, and G. Yu, "Parametric and working fluid analysis of a dual-loop organic Rankine cycle (DORC) used in engine waste heat recovery," *Appl. Energy*, vol. 113, 2014.

G. Manente, A. Lazzaretto, and E. Bonamico, "Design guidelines for the choice between single and dual pressure layouts in organic Rankine cycle (ORC) systems," *Energy*, vol. 123, pp. 413–431, 2017.

J. Li, Z. Ge, Y. Duan, and Z. Yang, "Design and performance analyses for a novel organic Rankine cycle with supercritical-subcritical heat absorption process coupling," *Appl. Energy*, vol. 235, pp. 1400–1414, Feb. 2019.

S. Rech, S. Zandarin, A. Lazzaretto, and C. A. Frangopoulos, "Design and off-design models of single and two-stage ORC systems on board a LNG carrier for the search of the optimal performance and control strategy," *Appl. Energy*, vol. 204, pp. 221–241, Oct. 2017.

T. Chen, W. Zhuge, Y. Zhang, and L. Zhang, "A novel cascade organic Rankine cycle (ORC) system for waste heat recovery of truck diesel engines," *Energy Convers. Manag.*, vol. 138, pp. 210–223, 2017.

T. Li, Z. Zhang, J. Lu, J. Yang, and Y. Hu, "Two-stage evaporation strategy to improve system performance for organic Rankine cycle," *Appl. Energy*, vol. 150, pp. 323–334, 2015.

S. Lecompte, H. Huisseune, M. Van Den Broek, and M. De Paepe, "Methodical thermodynamic analysis and regression models of organic Rankine cycle architectures for waste heat recovery," *Energy*, vol. 87, pp. 60–76, 2015.

U. Larsen, L. Pierobon, F. Haglind, and C. Gabrielii, "Design and optimisation of organic Rankine cycles for waste heat recovery in marine applications using the principles of natural selection," *Energy*, vol. 55, pp. 803–812, 2013.

C. Invernizzi, P. Iora, and P. Silva, "Bottoming micro-Rankine cycles for micro-gas turbines," vol. 27, pp. 100–110, 2007.